International Journal of Pharmaceutics 367 (2009) 51–57

Contents lists available at ScienceDirect

International Journal of Pharmaceutics

journal homepage: www.elsevier.com/locate/ijpharm

Characterisation and aerosolisation of mannitol particles produced via confined liquid impinging jets

P. Tang[a], H.-K. Chan[a,*], H. Chiou[a], K. Ogawa[a], M.D. Jones[b], H. Adi[a], G. Buckton[b], R.K. Prud'homme[c], J.A. Raper[d]

[a] Advanced Drug Delivery Group, Faculty of Pharmacy, The University of Sydney, New South Wales 2006, Australia
[b] Department of Pharmaceutics, The School of Pharmacy, University of London, 29-39 Brunswick Square, London WC1N 1AX, UK
[c] Department of Chemical Engineering, Princeton University, Princeton, NJ 08544, USA
[d] Department of Chemical and Biological Engineering, Missouri University of Science and Technology, Rolla, MO 65409, USA

ARTICLE INFO

Article history:
Received 24 April 2008
Received in revised form
12 September 2008
Accepted 12 September 2008
Available online 21 September 2008

Keywords:
Particle shape
Confined liquid impinging jet
Mannitol
Inhalation drug delivery
Inverse gas chromatography (IGC)

ABSTRACT

Mannitol particles, produced by spray drying (SD), have been used commercially (Aridol™) in bronchial provocation test. In this study, we propose an alternative method to produce inhalable mannitol powders. The elongated mannitol particles (number median length 4.0 μm, and axial ratio of 3.5) were prepared using a confined liquid impinging jets (CLIJs) followed by jet milling (JM). Spray dried and jet milled raw mannitol particles were compared in an attempt to assess the performance of the particles produced by the new method. Aerosol performance of the three different powders (CLIJ, SD, and JM) was relatively poor (fine particle fraction or FPF_{loaded} below 15%) when dispersed by the Rotahaler®. Dispersion through the Aeroliser® led to better aerosol performance of the CLIJ mannitol (FPF_{loaded} 20.3%), which is worse than the JM (FPF_{loaded} 30.3%) and SD mannitol particles (FPF_{loaded} 45.7%) at 60 L/min, but comparable (FPF_{loaded} 40.0%) with those of the JM (FPF_{loaded} 40.7%) and SD (FPF_{loaded} 45.5%) powders at 100 L/min. Hence, the optimum use of these elongated mannitol particles can be achieved at increased air flow with a more efficient inhaler. In addition to crystallinity, morphology, and particle size distribution, the surface energies of these powders were measured to explain the differences in aerosol performance. A major advantage of using the CLIJ method is that it can be scaled up with a good yield as the precipitate can be largely collected and recovered on a filter, compared with spray drying which has a low collection efficiency for fine particles below 2 μm.

1. Introduction

Mannitol is a sugar alcohol, and is used as a dry powder (Aridol™) by inhalation in bronchial provocation test (BPT) (Anderson et al., 1997; Brannan et al., 2005). Bronchial provocation test is conducted both to diagnose if a person has bronchial hyperresponsiveness and to assess the disease severity in asthmatic patients. Mannitol, inhaled into the airways, causes increase in the osmolarity of the fluid lining the mucosal surfaces. The bronchial muscle of an asthmatic person will contract with response to the rate of change of osmolarity. The change in osmolarity also induces mucous clearance and therefore may be beneficial for patients suffering from cystic fibrosis and chronic bronchitis (Daviskas et al., 1997, 1999, 2001, 2005; Robinson et al., 1999). Spherical mannitol particles used in Aridol™ were produced by spray drying (SD) (Chew and Chan, 1999). The aim of this study is to produce mannitol particles via an alternative method and to study their aerosol performance in comparison with particles obtained from other methods. In addition, we aimed to produce elongated particles with a high axial ratio, i.e., long thin needles, since thin elongated particles with a width below 1–2 μm and an axial ratio of minimum 10 will be aerodynamically small (Gonda and Abd El Khalik, 1985; Chan and Gonda, 1989a) and hence powder dispersion performance is potentially better. Aerodynamic diameter smaller than 5 μm is preferable for optimal lung deposition with minimal impaction in the upper airways. Gonda and co-workers first studied the aerodynamic properties of elongated drug particles in therapeutic aerosols during the early 1980s, including the free acid forms of cromoglycate and nedocromil (Chan and Gonda, 1989b; Chan and Gonda, 1995). The results confirmed that needle-shaped particles exhibit a low aerodynamic diameter. Hence, needle-like therapeutic particles are considered more likely to travel to the ciliated airways in the deeper lungs for optimum therapeutic benefit.

* Corresponding author. Tel.: +61 2 9351 3054; fax: +61 2 9351 4391.
E-mail address: kimc@pharm.usyd.edu.au (H.-K. Chan).

0378-5173/$ – see front matter © 2008 Elsevier B.V. All rights reserved.
doi:10.1016/j.ijpharm.2008.09.024

Our method involved precipitation by confined liquid impinging jet (CLIJ) precipitation from aqueous mannitol solution using acetone as an anti-solvent followed by filtration under high pressure, drying under vacuum and jet milling (JM) to break up the aggregates. The CLIJ technique, originally designed by Johnson and Prud'homme (2003a) has been used to produce organic and inorganic nanoparticles of salbutamol sulphate, cyclosporine (Chiou et al., 2008), β-carotene and polystyrene-block-poly (ethylene oxide) Johnson and Prud'homme (2003b). In principle, the CLIJ technique involves mixing two liquid streams in a single pass process to induce rapid mixing inside a small confined mixing vessel (Chiou et al., 2008).

In our study, the performance of spherical mannitol particles, produced by spray drying, and orthorhombic particles, obtained by jet milling of the commercially available raw mannitol powder, were compared to that of the needle-shaped particles produced by CLIJ. The morphology, crystal form and surface energy of each of these powders were examined by scanning electron microscopy, X-ray diffraction and inverse gas chromatography, respectively. Particle size of the SD mannitol was determined by laser diffraction. Particle size and shape (length, width and axial ratio) of the CLIJ and JM powders were measured by image analysis of scanning electron micrographs. The aerosol performance of each powder was assessed using two commercially available inhalers, the Rotahaler® and Aeroliser® dry powder inhalers connected to a multi-stage liquid impinger operating at flow rates of 60 (normal air flow that can be generated by a patient) and 100 L/min. With a large inspiratory effort (80 cm H_2O), a patient can generate 150 L/min through the Aeroliser® (Chew and Chan, 2001a). Even with a comfortable inspiratory effort of 40 cm H_2O, 105 L/min can still be generated through the Aeroliser®. Varying the inhaler device and air flow rate will give insight into the performance of the new powder since aerosol performance depends on these variables. Dispersive energies, obtained from inverse gas chromatography (IGC), together with the acceptor and donor numbers (K_A and K_B) were then used to explain the dispersion behaviour of the powders.

2. Methods and materials

2.1. Materials

Mannitol (Pearlitol® 160C) was obtained from Rocquette Frères, France. Acetone and isopropanol (both analytical grade) were supplied by Biolab Australia and plastic syringes (50 mL, 29.1 mm i.d.) were purchased from Livingstone Australia. Deionised water (>2 MΩ cm resistivity at 25 °C) was obtained from the Modulab Type II Deionization System (Continental Water Systems, Sydney, Australia). The following probes were used for IGC analysis: Acetone (high pressure liquid chromatography, HPLC grade), chloroform (HPLC grade), diethyl ether (AR grade), ethanol (HPLC grade), ethyl acetate (HPLC grade) and heptane (HPLC grade) were all obtained from Fisher Scientific (Loughborough, UK); Nonane (AR grade) was obtained from Acros Organics (Geel, Belgium) while acetonitrile (HPLC grade), decane (AR grade) and octane (AR grade) were from VWR (Poole, UK). Methane was supplied by BOC (Guildford, UK). All materials were used as received.

2.2. Methods

2.2.1. Preparation of mannitol powders by different methods

Elongated mannitol particles were obtained by mixing an aqueous solution of mannitol (5 mL, 0.18 g/mL) with acetone (40 mL) with the volume ratio set at 1:8, using CLIJ where the two liquid streams mixed inside a small confined mixing vessel, were flowing at rates of 15 and 120 mL/min, respectively. The resulting suspension was collected in a stainless steel pressure filtration unit (Sartorius, Germany) fitted with a 0.45 μm filter (Type HN, Millipore, US) and filtered using positive pressure (~1 bar) to form a soft and light cake, which was then dried in a vacuum oven (OVL-570, Gallenkamp, UK) at 30 °C and 1000 mbar for 18 h. To obtain the fine powder, the dried cake was loosely broken up with a mortar and pestle then fed into an air jet mill (Gem-T Research Model, Trost Equipment Corporation, USA), using a feed pressure of 40 psi and a grinding pressure of 100 psi.

Spherical mannitol particles were obtained by spray drying (Büchi 191, Flawil, Switzerland) with a feed concentration of 10 mg/mL, with inlet and outlet temperature, 110 and 75 °C, respectively, a feed rate of 1.4 mL/min, aspiration set at maximum (i.e., 38 m^3/h) and an atomising air rate of 800 NL/h.

Orthorhombic shaped mannitol particles were obtained by air jet milling the starting commercial mannitol powder with a feed pressure of 40 psi and a grinding pressure of 100 psi. All powders produced by CLIJ, spray drying, and jet-milling methods were stored in a desiccator box until use.

2.2.2. Powder crystallinity and polymorphism

Powder crystallinity and polymorphism was assessed by X-ray diffraction (XRD, D5000, Siemens, Germany) conducted at room temperature using Cu Kα radiation at 30 mA and 40 kV, with an angular increment of 0.05°/s and count time of 2 s from 2-theta of 9–40°.

2.2.3. Microscopy and particle size distribution

The morphology of the mannitol particles was examined by high-resolution scanning electron microscopy (SEM, JSM 6000F, Joel, Japan) operating at 3.0 kV. The particle size distribution of the spray-dried powder was determined by connecting a wet disperser (Hydro SM, Malvern, Worcs, UK) to a laser diffractometer (Mastersizer 2000, Malvern, Worcs, UK) based on the refractive indices of mannitol (1.520 and 0.100 for real and imaginary components, respectively) and the dispersing medium, chloroform (1.444). It is not appropriate to measure the size distribution of elongated and orthorhombic particles by laser diffraction using Mie's theory because it assumes measured particles are spherical, so size distributions based on length, width and axial ratio of the orthorhombic and elongated mannitol were obtained by image analysis of SEM images (ImageJ, Rasband, 1997–2006). The length was defined as the longest dimension of the particle and the width as the second longest dimension. CLIJ and JM mannitol particles were suspended in cyclohexane (3 mg/mL), spread onto a copper plate and coated with a 50 nm platinum layer for observation. To ensure the size distributions were representative of the powder, random samples were taken. A random list of x and y coordinates was generated by a random number generator (Minitab, release 13 for Windows, Minitab Inc., USA). A total of 60 fields of view were selected for examination, with a minimum total number of 200 particles measured for each sample.

2.2.4. Surface energy determination by inverse gas chromatography

IGC experiments were performed using the commercial IGC system (Surface Measurement Systems, London, UK) with a research grade helium carrier gas flow (BOC, Guildford, UK) of 30 mL/min in a dry atmosphere. Adsorbate injections were carried out at the minimum concentration allowed by the IGC control software. Measurements were carried at 303 K. Each new column was allowed to equilibrate to the IGC conditions for 7 h (JM and SD mannitol samples) or 11 h (CLIJ mannitol samples) before injections commenced. An equilibration time of 60 min was allowed following

column oven temperature changes with a 30 min wait between injections. 300 mm silanised glass columns of 3 mm (SD and CLIJ mannitol) or 4 mm (JM mannitol) internal diameter (Surface Measurement Systems, London, UK) were packed with an appropriate mass of powder (~1.2 g for JM mannitol, ~0.21 g for SD mannitol and ~0.16 g for CLIJ mannitol). The column ends were plugged with silanised glass wool. Columns of JM and CLIJ mannitol were tapped for 15 min on a jolting voltameter (Surface Measurement Systems, London, UK) to ensure uniform column packing. Spray dried materials can be too tightly packed to allow the passage of the carrier gas if treated in this way, so the SD mannitol columns were tapped by hand 10 times. Two columns of each material were used with the chosen series of adsorbates injected into each column twice. Thus four sets of dispersive surface energies were obtained for each material. Raw data were analysed using IGC Analysis Macros (v1.3 standard edition, Surface Measurement Systems, London, UK) to calculate the dispersive surface tension at each temperature and the acceptor and donor numbers were calculated by the Schultz method (Schultz et al., 1987).

2.2.5. Aerosol performance

The dispersion behaviour of the powders was assessed using a Rotahaler® (Allen & Hanburys, Australia) or an Aeroliser® (Novartis Pharmaceuticals, Australia) coupled through an USP stainless steel throat to a multi-stage liquid impinger (MSLI, Copley, UK), operating at flow rates of 60 and 100 L/min. A single experiment comprised of two capsules and two experiments were conducted. Mannitol powder (20.0 ± 0.5 mg) was filled into hydroxypropyl methylcellulose capsules (size 3, Capsugel®, USA). Mannitol deposited at each location was assayed by high performance liquid chromatography (Waters, USA) using refractive index detection (410 differential refractometer, Waters, USA). Samples were injected (100 μL) into a C18 Radial-Pak column (Waters, USA) with de-ionised water as the mobile phase running at a flow rate of 1 mL/min for 6 min and a retention time of around 3 min. A calibration curve was constructed using standard solutions of mannitol (from 0.1 to 10 mg/mL), allowing the mass of powder deposited at each location to be determined. Fine particle fraction (FPF) is defined as the mass fraction of drug particles smaller than 5 μm in the aerosol cloud (interpolated from the mass of drug collected from stages 3, 4 and filter) relative to the total mass loaded to (FPF_{loaded}) or emitted from ($FPF_{emitted}$) the device. The particle size cut-offs (D) of the MSLI were corrected for differences in flow rates (Q) using the following relationship $D_2 = D_1\sqrt{Q_1/Q_2}$.

3. Results and discussion

3.1. Powder crystallinity and polymorph

The mannitol samples were found to be crystalline, as shown by X-ray diffraction patterns of the three powders showing strong peaks (Fig. 1). The X-ray diffraction patterns of both JM and SD powders are almost identical (Fig. 1A and B) with the peak positions corresponding to the D-β-mannitol polymorph (like the raw material, data not shown), while the diffraction patterns of the CLIJ powder (Fig. 1C) corresponds predominately to D-α-mannitol (Kim et al., 1998). Both the α and β polymorphs are considered stable (Kim et al., 1998; Burger et al., 2000).

3.2. Powder morphology and size

The needle-shaped mannitol particles were obtained by mixing an aqueous solution of saturated mannitol with pure acetone with volume ratios more than 1–5. As the volume of acetone increases

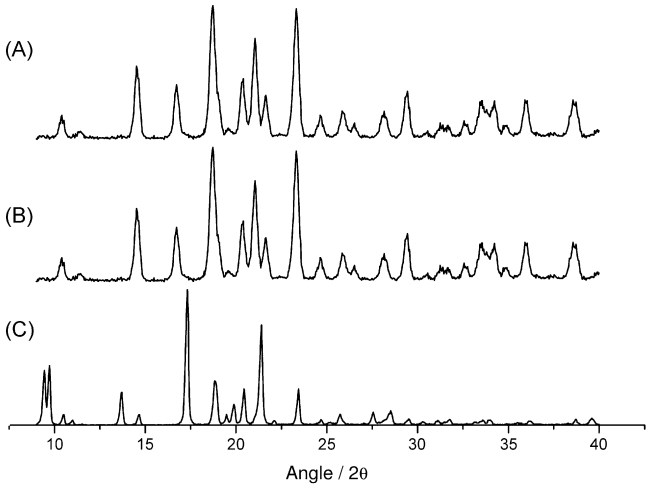

Fig. 1. X-ray diffraction pattern of (A) jet milled raw, (B) spray dried and (C) CLIJ precipitated mannitol.

the particles tend to become thinner and longer until they reach an optimum point. There was no significant difference in axial ratio when the volume of acetone was increased to give a ratio of 1:8. When the volume ratio was increased to 1:20, the needle-shaped particles became significantly shorter. The morphology of the needle particles immediately after they were formed, as observed under optical microscope Olympus CH40, is shown in Fig. 2. In general, the particles were thin (width approximately 1–2.5 μm) and long, with no plate-like (i.e., short axial ratio) elongated particles observed.

Fig. 3 shows the orthorhombic, spherical and needle-shaped particles of mannitol, produced by jet milling, spray drying and confined impinging jet precipitation followed by drying and jet milling, respectively. The drying process changed the axial ratio of the elongated particles obtained by the CLIJ technique (Fig. 3C). Various methods of filtration, namely gravity, vacuum, high pressure, were found to cause the needle-shaped particles to break up. The jet-milling process that followed the high-pressure filtration cut the particles into shorter needles, resulting in a smaller axial

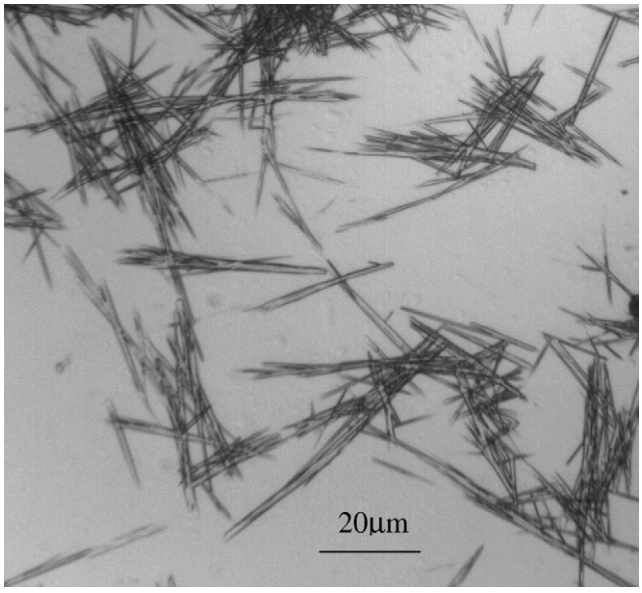

Fig. 2. Needles mannitol particles obtained via confined liquid impinging jet techniques. Ratio of saturated mannitol solution to acetone is 1:8.

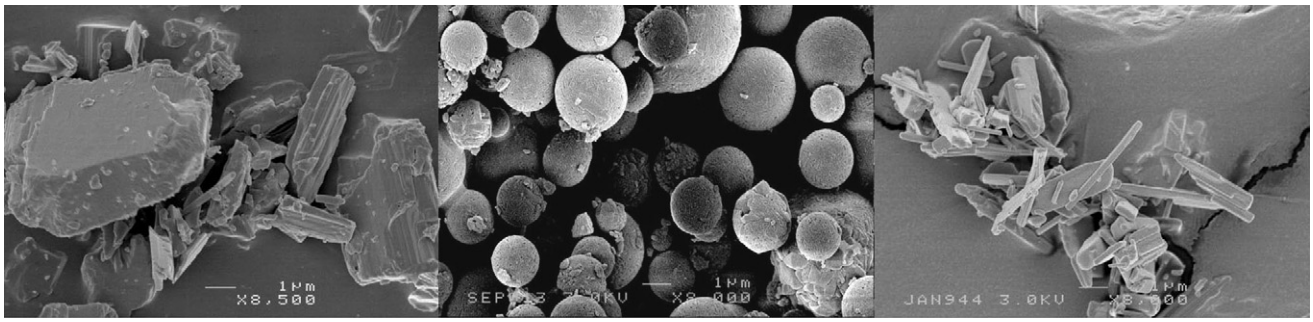

Fig. 3. SEM images of (A) jet milled raw, (B) spray dried and (C) CLIJ precipitated mannitol.

ratio than the original long and thin particles. The high-pressure filtration was chosen because it is the fastest process compared to the vacuum and gravity filtrations, and hence any formation of solid bridging between particles that can affect the dispersibility of the powder was minimised.

The median length of the CLIJ mannitol is longer than the JM mannitol particles (Fig. 4A), the width of the CLIJ particles is slightly higher (Fig. 4B) and the axial ratio is twice that of the JM particles (Fig. 4C).

3.3. Surface energy

Surface energy is particularly useful in the present study as it reflects variations in the crystal habit or polymorphic form among the samples. The surface energies of mannitol were found to be different among the three samples. As shown in Table 1, the elongated mannitol has significantly higher dispersive energies, hence being more cohesive, compared with the JM or SD mannitol samples. While the difference in the surface energies between the JM and SD mannitol is due to a change in the crystal habit, the higher energy of the CLIJ mannitol may be because it is a different polymorph. The acceptor (acidic, K_A) and donor (basic, K_B) numbers

Table 1
Dispersive energies and acceptor and donor indexes (K_A and K_B) of the different mannitol powders at 303 K.

Mannitol	Dispersive energy (mJ M^2)	K_A	K_B
Jet milled	47.92 ± 1.35	0.14 ± 0.02	0.26 ± 0.12
Spray dried	60.27 ± 0.96	0.29 ± 0.04	0.16 ± 0.23
CLIJ	85.28 ± 2.35	0.25 ± 0.05	0.26 ± 0.29

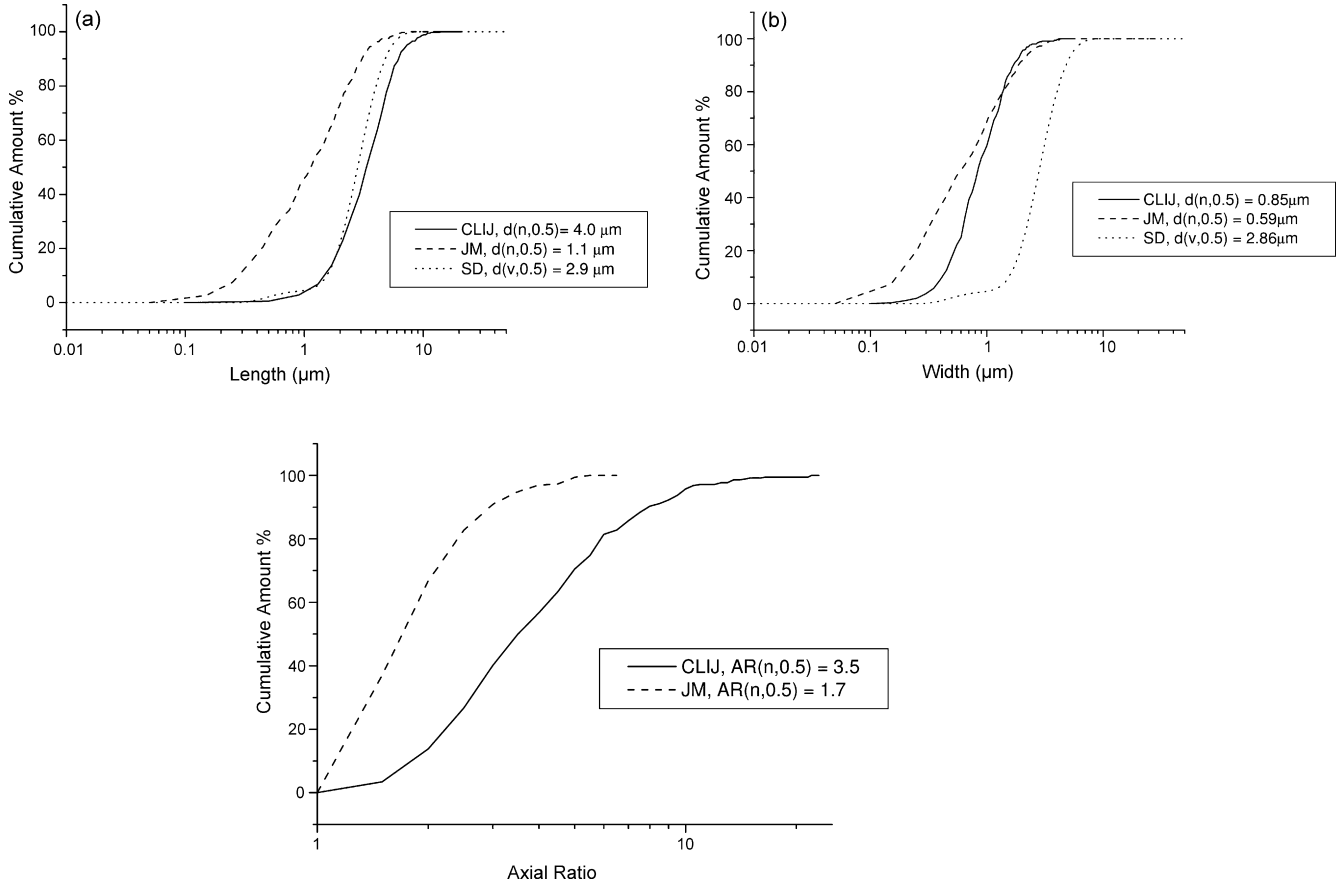

Fig. 4. Cumulative distributions for (A) length, (B) width and (C) axial ratio. As the spray dried powder are spherical, the length and width distributions are the same and the axial ratio equals to one.

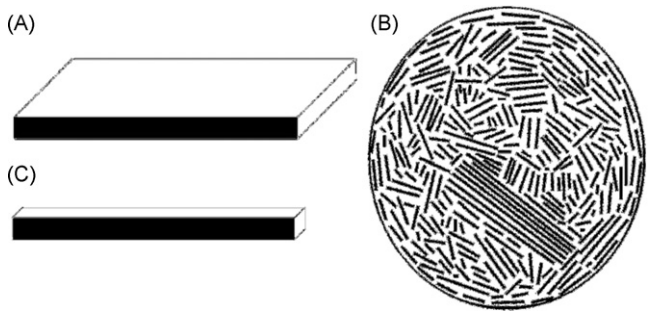

Fig. 5. Schematic diagram showing the exposed faces of (A) JM mannitol, (B) SD mannitol and (C) CLIJ mannitol. Black shading or lines represent faces that are strong electron acceptors.

show the majority of the JM mannitol surface being strong electron donating while SD mannitol being predominantly electron accepting. Interestingly, CLIJ mannitol has both types of surfaces, implying the potential of electron donor–acceptor interactions between the particle surfaces and such non-dispersive interactions may further contribute to the cohesion between these elongated particles.

In studies on paracetamol, Heng et al. (2006) showed that the values of K_A or K_B depend on which crystal face is exposed. The values obtained by IGC for the three powders suggest that some faces of the mannitol crystal are strong acceptors while the others are donors, as schematically represented in Fig. 5: (A) predominantly electron-donor faces exposed in the JM mannitol crystals; (B) electron-acceptor faces of the SD mannitol particle comprising small (poly)crystals; (C) similar 'effective' areas of both electron-donor and acceptor faces exposed in the elongated CLIJ crystals, leading to similar acceptor and donor numbers. As the CLIJ mannitol is a different polymorph, it will have different faces compared to JM and SD mannitol, which may also contribute to the K_A and K_B differences.

3.4. Aerosol performance

The *in vitro* aerosol performance of the powders was examined using two commercial devices (Rotahaler® and Aeroliser®) each having different efficiencies in dispersing the powder, at two flow rates (60 and 100 L/min). Relatively speaking, the Rotahaler® and the Aeroliser® (similar to the Dinkihaler® from Aventis) (Chew and Chan, 2002; Coates et al., 2004, 2005a,b, 2006) are of low and high dispersion efficiency, respectively.

Elongated mannitol was very poorly dispersed (FPF_{loaded} < 5%) using the Rotahaler®, as were the orthorhombic and spherical particles (FPF_{loaded} < 5 and 15%, respectively). These low values are not due to the high device and capsule retention shown in Table 2, because the $FPF_{emitted}$ results are also consistently low. The poor

Table 2
Mass retained (%) within the device and capsule as well as deposited in the throat.

Powder (flow rate) and device	Device	Capsule	Throat
CLIJ (60 L/min) Rotahaler®	6.84, 7.04	0.15, 0.31	2.25, 2.35
CLIJ (100 L/min) Rotahaler®	11.4, 13.6	0.25, 0.27	2.53, 2.85
CLIJ (60 L/min) Aeroliser®	45.1, 44.5	8.79, 10.6	5.44, 4.57
CLIJ (100 L/min) Aeroliser®	16.8, 17.4	3.29, 5.45	18.5, 18.9
JM (60 L/min) Rotahaler®	13.7, 16.1	0.82, 1.68	3.92, 4.14
JM (100 L/min) Rotahaler®	18.3, 22.9	1.46, 1.66	5.58, 7.62
JM (60 L/min) Aeroliser®	29.5, 31.5	13.3, 13.5	8.73, 9.05
JM (100 L/min) Aeroliser®	14.8, 15.0	3.28, 7.72	19.3, 22.1
SD (60 L/min) Rotahaler®	17.7, 21.2	4.45, 6.51	3.56, 3.66
SD (100 L/min) Rotahaler®	16.0, 17.2	1.52, 6.50	8.06, 9.86
SD (60 L/min) Aeroliser®	14.8, 16.0	2.98, 1.70	9.83, 7.94
SD (100 L/min) Aeroliser®	6.43, 6.41	1.52, 1.86	18.7, 20.3

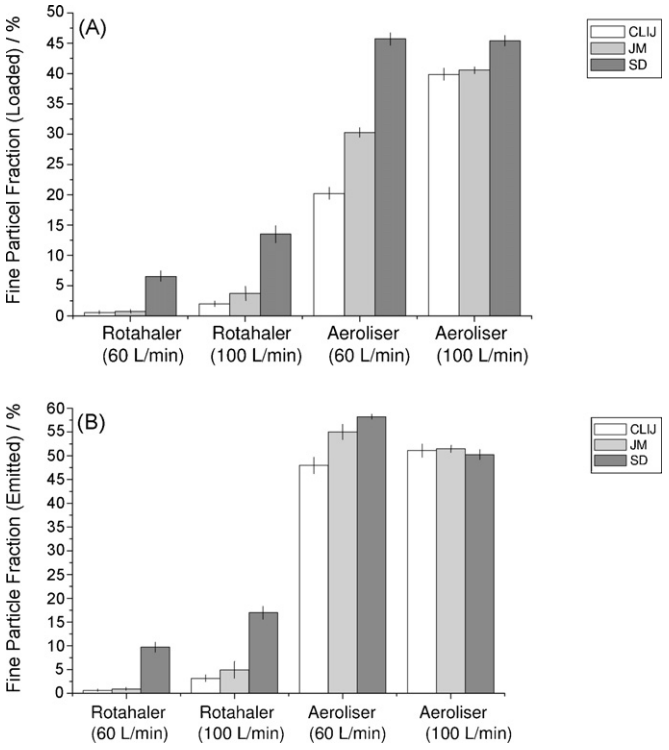

Fig. 6. Fine particle fractions relative to (A) recovered mass, and (B) emitted mass of the mannitol powders (white, CLIJ; light gray, JM; and dark gray, SD). Vertical lines show the value range of results (not standard deviation) from the two runs.

performance of the Rotahaler® is well known (Chew and Chan, 1999; Chew et al., 2000), however, the inhaler can still generate a FPF above 30% for powders that are less cohesive (Chew and Chan, 2001b). Together with the air flow dependence of the FPF, the results show that these powders are cohesive and this inhaler could not sufficiently overcome the inter-particulate interactions. Overall, CLIJ mannitol had the lowest FPF, despite having the narrowest particles with the largest axial ratio. The cohesion of the elongated mannitol is due to the high surface energy, high surface-to-volume ratio and potentially closer packing of the needles along their long axis, or a combination of these factors. Interestingly, despite having higher surface energy, the SD mannitol dispersed better than the JM mannitol. This can be attributed to the contact area between the spherical particles being less than the orthorhombic ones, and that the spheres can better deagglomerate by the additional mechanism of rolling. Although the contact area of spherical powders is generally low, in these cases where elongated particles can preferentially align along the axis, the contact area can be much greater than that of the spherical powder.

Dispersion of the elongated mannitol was much improved (FPF_{loaded} ~ 20–40%) using the Aeroliser® (Fig. 6A). The lower FPF_{loaded} of 20.2% (19.2%, 21.2%) at 60 L/min can be explained by the high device and capsule retention of 54.5% (53.9%, 55.1%, Table 2), which, in turn, is ascribable to the enhanced adhesion of these more energetic needles having high surface-to-volume ratio interacting with the inhaler and capsule surfaces. This is further supported by the lack of air flow dependence in the $FPF_{emitted}$ results (Fig. 6B), i.e., once emptied from the device, the powder shows good quality ($FPF_{emitted}$ ~ 50%) in the emitted aerosol cloud. At 100 L/min, the increasing dispersion energy overcomes both the powder adhesion and cohesion, leading to a reduced device and capsule retention of 21.4% (20.3%, 22.5%) (Table 2) and a concomitant increase in the FPF_{loaded} to 39.9% (38.9%, 40.9%). The dispersion and retention

behaviour of the orthorhombic mannitol is qualitatively similar to the mannitol needles. The higher FPF_{loaded} of 30.3% (29.5%, 31.1%) at 60 L/min can be readily attributed to the lower surface energy along with the lower surface-to-volume ratio of these particles (hence less adhesive to the device surfaces) than those of the needles. In contrast, the spherical mannitol does not show any flow dependence of the FPF, indicating the powder is least adhesive and cohesive, which may be a result of a lower contact area between spheres, easier detachment and deagglomeration due to potential rolling action coupled with a larger gravitational force because of larger particle size (hence bigger mass), and medium surface energy.

While the above discussion focuses on the powder adhesion and dispersion of the CLIJ, SD and JM mannitols, it is important to note that once the particles are airborne, the difference in the particle shape and size would also affect the aerodynamic diameter (Da) and hence the FPF (Chan, 2007). It is difficult to calculate the Da of the JM mannitol due to the large variation in the particle shape and the uncertainty in the dynamic shape factor. However, it is possible to obtain the theoretical Da of the elongated CLIJ mannitol using the Harris and Fraser expression modified by Gonda and Abd El Khalik (1985). The theoretical calculation showed a mass median aerodynamic diameter of 2.01 μm with a geometric standard deviation of 1.54. These results have been based on complete dispersion of the powder into aerosol particles. In practice, this was not the case as shown in the experimental data. Had the powder been fully dispersed, the CLIJ mannitol would have been aerodynamically smaller than the SD mannitol. The actual effect of particle size distribution on the aerosol behaviour is unknown, and the amount of data in the literature is scarce. Our previous results showed that for the SD mannitol, decreasing the polydispersity of the powder generated more fine particles by the Rotahaler® at medium flows (60 and 90 L/min), but polydispersity had no effect when the powder was dispersed by the Aeroliser® (Chew and Chan, 2002).

4. Conclusions

Our results have provided clear evidence to show that the confined liquid impinging jet (CLIJ) technique can be a suitable alternative method to produce particles for inhalation. It has been shown to successfully produce elongated mannitol particles with axial ratios greater than 10. The subsequent processes to dry and breakup the aggregates to form dispersible powders including filtration under high pressure, drying under vacuum, and jet milling were shown to shorten the axial ratio to approximately 3.5. Our results have indicated that these elongated particles have small aerodynamic diameters suitable for pulmonary delivery. Mannitol particles of other shapes, namely orthorhombic and spherical—were also produced. Particle shape is an important contributor to the aerosol performance of mannitol powders as it affects the surface energy and particle dynamics (contact area, packing and detachment). Differences in the dispersion behaviour between mannitol samples are not sufficiently accounted for by surface energy alone, indicating that particle dynamics also play a key role. The CLIJ mannitol particles were found to be the most cohesive and adhesive. However, these particles can perform as well as other types of mannitol particles using an Aeroliser® at 100 L/min, an air flow rate which is readily achievable by patients (Clark and Hollingworth, 1993; Glover et al., 2006). The aerosol performance of the CLIJ mannitol particles is reduced at low flow rates, or when a less efficient inhaler was used. As mentioned before, the CLIJ method is easy to scale up with a good yield as the precipitate can be largely collected and recovered on the filter, compared with spray drying which has a low collection efficiency for fine particles below 2 μm.

Acknowledgements

This work was supported by a grant from the Australian Research Council (DP 0451940). One of the authors (JAR) is located at the National Science Foundation (NSF). Any opinion, findings, and conclusions or recommendations expressed in this material are those of the authors and do not necessarily reflect the views of the National Science Foundation. MDJ gratefully acknowledges financial support in the form of a Maplethorpe Trust Fellowship.

References

Anderson, S.D., Brannan, J., Spring, J., Spalding, N., Rodwell, L.T., Chan, H.-K., Gonda, I., Walsh, A., Clark, A.R., 1997. A new method for bronchial-provocation testing in asthmatic subjects using a dry powder of mannitol. Am. J. Respir. Crit. Care 156, 758–765.

Brannan, J., Anderson, S.D., Perry, C.P., Freed-Martens, R., Lassig, A.R., Charlton, B., 2005. The safety and efficacy of inhaled dry powder mannitol as a bronchial provacation test for airway hyperresponsiveness: a phase 3 comparision study with hypertonic (4.5%) saline. Respir. Res. 6, 144.

Burger, A., Henck, J.-O., Hetz, S., Rollinger, J.M., Weissnicht, A.A., Stottner, H., 2000. Energy/temperature diagram and compression behavior of the polymorphs of D-mannitol. J. Pharm. Sci. 89, 457–468.

Chan, H.K., Gonda, I., 1989a. Aerodynamic properties of elongated particles of cromoglycic acid. J. Aerosol Sci. 20, 157–168.

Chan, H.K., Gonda, I., 1989b. Respirable form of crystals of cromoglycic acid. J. Pharm. Sci. 78, 176–180.

Chan, H.-K., Gonda, I., 1995. Physicochemical characterization of a new respirable form of nedocromil. J. Pharm. Sci. 84, 692–696.

Chew, N.Y.K., Chan, H.K., 1999. Influence of particle size, air flow, and inhaler device on the dispersion of mannitol powders as aerosols. Pharm. Res. 16, 1098–1103.

Chew, N.Y.K., Bagster, D.F., Chan, H.K., 2000. Effect of particle size, air flow and inhaler device on the aerosolisation of disodium cromoglycate powders. Int. J. Pharm. 206, 75–83.

Chew, N.Y.K., Chan, H.-K., 2001a. In vitro aerosol performance and dose uniformity between the Foradile Aeroliser and the Oxis Turbuhaler. J. Aerosol Med. 14, 495–501.

Chew, N.Y.K., Chan, H.K., 2001b. Use of solid corrugated particles to enhance aerosol performance. Pharm. Res. 18, 1570–1577.

Chew, N.Y.K., Chan, H.K., 2002. Effect of powder polydispersity on aerosol generation. J Pharm. Pharm. Sci. 5, 162–168.

Chan, H.K., 2007. In: Dalby, R.N., Byron, P.R., Peart, J., Suman, J. D. (Eds), The Role of Particle Morphology in Powder Inhalers. Respiratory Drug Delivery Europe, Paris. Davis Healthcare International Publishing, River Grove, IL, p. 187–196.

Chiou, H., Chan, H.-K., Prud'homme, R.K., Raper, J.A., 2008. Evaluation on the use of confined liquid impinging jets for the synthesis of nanodrug particles. Drug Dev. Ind. Pharm. 34, 59–64.

Clark, A.R., Hollingworth, A.M., 1993. The relationship between powder inhaler resistance and peak inspiratory conditions in healthy volunteers—implications for in-vitro testing. J. Aerosol Med. 6, 99–110.

Coates, M.S., Chan, H.-K., Fletcher, D.F., Raper, J.A., 2004. Effect of design on the performance of a dry powder inhaler using computational fluid dynamics. Part 1. Grid structure and mouthpiece length. J. Pharm. Sci. 93, 2863–2876.

Coates, M.S., Chan, H.-K., Fletcher, D.F., Raper, J.A., 2005a. The influence of air flow on the performance of a dry powder inhaler using computational and experimental analyses. Pharm. Res. 22, 1445–1453.

Coates, M.S., Chan, H.-K., Fletcher, D.F., Raper, J.A., 2005b. The role of capsule on the performance of a dry powder inhaler using computational and experimental analyses. Pharm. Res. 22, 923–932.

Coates, M.S., Chan, H.-K., Fletcher, D.F., Raper, J.A., 2006. Effect of design on the performance of a dry powder inhaler using computational fluid dynamics. Part 2. Air inlet size. J. Pharm. Sci. 95, 1382–1392.

Daviskas, E., Anderson, S.D., Brannan, J.D., Chan, H.-K., Eberl, S., Bautovich, G., 1997. Inhalation of dry-powder mannitol increases mucociliary clearance. Eur. Respir. J. 10, 2449–2454.

Daviskas, E., Anderson, S.D., Eberl, S., Chan, H.-K., Bautovich, G., 1999. Inhalation of dry powder mannitol improves clearance of mucus in patients with bronchiectasis. Am. J. Respir. Crit. Care 159, 1843–1848.

Daviskas, E., Anderson, S.D., Eberl, S., Chan, H.-K., Young, I.H., 2001. The 24-h effect of mannitol on the clearance of mucus in patients with bronchiectasis. Chest 119, 414–421.

Daviskas, E., Anderson, S.D., Gomes, K., Briffa, P., Cochrane, B., Chan, H.-K., Bautovich, G., 2005. Inhaled mannitol for the treatment of mucociliary dysfunction in patients with bronchiectasis—effect on lung function. Health status and sputum. Respirology 10, 46–56.

Glover, W., Chan, H.-K., Eberl, S., Daviskas, E., Anderson, S., 2006. Lung deposition of mannitol powder aerosol in healthy subjects. J. Aerosol Med. 19, 522–532.

Gonda, I., Abd El Khalik, A.F., 1985. On the calculation of aerodynamic diameters of fibers. Aerosol Sci. Technol. 4, 233–238.

Heng, J.Y.Y., Thielmann, F., Williams, D.R., 2006. The effects of milling on the surface properties of form I paracetamol crystals. Pharm. Res. 23, 1918–1927.

Johnson, B.K., Prud'homme, R.K., 2003a. Chemical processing and micromixing in confined impinging jets. AIChE J. 49, 2264–2282.
Johnson, B.K., Prud'homme, R.K., 2003b. Flash nanoprecipitation of organic actives and block copolymers using a confined impinging jets mixer. Aust. J. Chem. 56, 1021–1024.
Kim, A.I., Akers, M.J., Nail, S.L., 1998. The physical state of mannitol after freeze-drying: effects of mannitol concentration, freezing rate, and a noncrystallizing cosolute. J. Pharm. Sci. 87, 931–935.
Rasband, W.S., 1997–2006. ImageJ (http://rsb.info.nih.gov/ij/), U.S. National Institutes of Health, Bethesda, MD, USA.
Robinson, M., Daviskas, E., Eberl, S., Baker, J., Chan, H.-K., Anderson, S.D., Bye, P.T., 1999. The effect of inhaled mannitol on bronchial mucus clearance in cystic fibrosis patients: a pilot study. Eur. Respir. J. 14, 678–685.
Schultz, J., Lavielle, L., Martin, C., 1987. The role of the interface on carbon fiber-epoxy composites. J. Adhes. 23, 45–60.